Low-Noise Performance Near BV_{CEO} in a 200 GHz SiGe Technology at Different Collector Design Points

D. Greenberg#, S. Sweeney*, G. Freeman and D. Ahlgren
IBM Microelectronics, 2070 Rt. 52, Hopewell Junction, NY 12533 *Burlington, VT
#IBM Research, Yorktown Heights, NY
Email: drgreen@us.ibm.com Phone/Fax: 845-892-2510/3039

Abstract – We explore the low-noise behavior of both high-f_T and enhanced-breakdown SiGe HBTs, showing key differences as a function of V_{CB}. Both devices achieve values for F_{min} below 0.4, 1.2 and 1.4 dB at 10, 15 and 20 GHz, respectively, with corresponding G_A values better than 18.5, 14.5 and 13.2 dB. In addition, the enhanced-breakdown device demonstrates the ability to operate at 1 V higher V_{CB} compared with the high-f_T device prior to the onset of avalanche-induced F_{min} degradation. Combined with a lower C_{CB}, this improved V_{CB} range allows the device to achieve higher gain for the same or lower noise.

I. INTRODUCTION

As SiGe HBT performance has progressed in recent years from below 50 GHz to beyond 300 GHz, a collection of applications requiring high-speed devices has evolved in parallel. One such collection is wired networking at increasing faster bit rates. Building blocks for 40 Gb/s systems have, for example, been implemented successfully in 120 GHz SiGe BiCMOS [1].

In addition to wired applications, however, there are also emerging wireless markets at higher frequencies, from cordless telephony at 5.8 GHz to wireless LAN and collision avoidance radar in the 60-77 GHz spectrum. Evaluating new technologies for these applications requires looking at RF figures of merit beyond f_T and f_{MAX}, such as noise performance. SiGe HBTs have demonstrated excellent low-noise capabilities due to their combination of high f_T, high current gain (β) and low base resistance (R_B) [2]. Most recently, IBM has reported a SiGe HBT technology with f_T and f_{MAX} greater than 200 GHz capable of low noise figure (F_{min}) and high associated gain (G_A) out to at least 26 GHz [3]. This domain has, until recently, been exclusive to III-V devices, particularly GaAs PHEMTs.

The availability of a silicon solution for low noise at high frequencies enables system-level integration. A SiGe device library may include several active device types that can be combined in the same circuit, each tailored to specific design goals. For example, in addition to a high-f_T device, a SiGe HBT library may include variants that trade f_T for breakdown voltage. Such a device might be achieved by reducing or eliminating the doping in the collector pedestal, improving breakdown in exchange for an earlier onset of the Kirk effect and thus for a lower peak f_T. Since a SiGe HBT generally exhibits optimum noise properties at less than 10% of peak-f_T current (referenced to the high-f_T variant), there is margin for an earlier Kirk effect onset without impacting f_T at typical low noise biases. Indeed, doing so could result in achieving lower noise. Reducing the collector doping decreases the collector-base capacitance (C_{CB}), improving gain. Base depletion is also reduced, lowering R_B and thus F_{min}.

Further, while breakdown voltage as a measure of the safe operating area of a device is generally accepted, the designer may care about additional considerations in low noise design. Since the physical mechanism for breakdown in an HBT is avalanche, an inherently random phenomenon, noise can increase at collector-base voltages (V_{CB}) below breakdown, even if avalanche is not yet sufficiently strong to show evidence in the I-V curves. The resulting performance drop sets an effective upper voltage limit for low-noise operation beyond that determined by the I-V curves alone. This knowledge of the noise behavior of an HBT in the vicinity of breakdown, including comparison between the high-f_T and enhanced-breakdown devices, is valuable information to the circuit designer.

This work explores for the first time the noise behavior as a function of V_{CB} of two types of HBTs built in IBM's 200 GHz SiGe HBT technology: a flagship high-f_T device as well as an experimental enhanced-breakdown variant. The results reveal the impact of avalanche on noise. We report that the enhanced-breakdown device is particularly attractive for low-noise, showing identical or better noise figure to the high-f_T device while demonstrating reduced avalanche-induced noise and thus permitting operation at higher V_{CB} values for higher gain.

II. TECHNOLOGY AND EXPERIMENTAL SETUP

The vehicle for our study is IBM's 200 GHz SiGe HBT, illustrated in Fig. 1, featuring a raised extrinsic base self-aligned to an in-situ-doped emitter [4]. In contrast with prior SiGe generations sharing a common film for intrinsic and extrinsic base, the raised extrinsic base permits heavier doping for a large reduction in R_B while maintaining low C_{CB} and thus high power gain and f_{MAX}. By modifying the collector implant selectively, we create two HBT variants. The typical f_T and f_{MAX} performance of the flagship device (highest collector doping) is shown in Fig. 2. Peak f_T and f_{MAX} (from unilateral gain) values are 200 GHz and 250 GHz, respectively. We also explore an HBT variant with reduced collector doping achieving the f_T and f_{MAX} performance shown in Fig. 3. For this variant, the onset of the Kirk effect, and thus the peak-f_T current, varies considerably with V_{CB}. This V_{CB} dependence is most pronounced between 0 V and 1 V, tapering off by 1.5 V where the peak f_T and f_{MAX} values are 75 GHz and 200 GHz, respectively. We note that f_{MAX}, arguably more critical than f_T for RF applications, is high despite lower f_T as a result of greatly reduced C_{CB}. Fig. 4 illustrates the forced-I_B output curves of both variants for identical I_B steps. The high-f_T HBT shows greater I_C with a BV_{CEO} of 1.8 V, while the modified-collector device shows reduced I_C but an improved BV_{CEO} of 2.8 V.

All devices were tested on-wafer in an ATN noise characterization system at 10, 15 and 20 GHz and over a range of I_C and V_{CB} values. Pad calibration structures were measured as well, allowing de-embedding of pad parasitics. All f_T, f_{MAX} and I-V data was taken on devices with an emitter area of 0.12 x 2.5 μm^2, while noise characterization was performed using larger 0.12 x 20 μm^2 devices more typical to low-noise design.

III. EXPERIMENTAL RESULTS

Figs. 5 and 6 illustrate typical F_{min} and G_A performance vs. I_C between 0.5 and 8 mA for both HBT variants at 10, 15 and 20

0-7803-7695-1/03/$17.00 © 2003 IEEE

GHz. Since I_B remains below 3% of I_C under all test conditions, I_C can be considered equal to I_E. To establish a baseline for noise in the technology, we focus initially on V_{CB} = 1 V, a bias below breakdown in either device yet above the value at which the enhanced-breakdown device shows large V_{CB} dependence in f_T and f_{MAX}. For the high-f_T device, the best observed F_{min} values at 10, 15 and 20 GHz are 0.4, 1.2 and 1.4 dB, with corresponding best G_A of 18.5, 14.5 and 13.2 dB. In comparison, the enhanced-breakdown device actually shows about 0.1 dB lower F_{min} and 0.7 dB higher G_A at all three frequencies. This behavior reveals the benefits of trading f_T at currents outside the needs of the application for lower C_{CB} and R_B.

Exploring noise performance as a function of V_{CB} reveals additional differences between the two device variants. Finding qualitative behavior to be identical at all measured frequencies, we take a detailed look at the data for 15 GHz. Fig. 7 plots F_{min} vs. I_C between 0.5 and 8 mA for the high-f_T device variant for a range of V_{CB} values from 0 to 1.75 V. Since V_{BE} is approximately 0.8 V over the tested I_C range, V_{CE} spans from 0.8 to 2.55 V. This range covers the region below, through and beyond BV_{CEO}, permitting us to explore the impact of avalanche on noise as we cross through this voltage limit benchmark. We note that F_{min} shows little dependence on V_{CB} for values of 0.75 V and below, with the data traces overlaying. However, F_{min} rises by up to 0.1 dB once V_{CB} reaches 1 V (corresponding to $V_{CE} = BV_{CEO}$), with the degradation increasing as a function of I_C. The increase in F_{min} with V_{CB} becomes more dramatic with still higher V_{CB}, reaching 1.0 dB at V_{CB} = 1.75 V for an I_C of 6 mA.

In contrast, the enhanced-breakdown device shows little such increase in F_{min} with V_{CB}, as illustrated in Fig. 8 for V_{CB} values up to 2 V. In fact, the first noticeable rise in F_{min} occurs at V_{CB} = 2 V, a full volt higher than the point of similar degradation in the high-f_T device. This improvement in V_{CB} dependence is consistent with the 1 V difference in BV_{CEO} values. While the enhanced-breakdown variant shows immunity against increasing noise at high V_{CB}, it suffers from a phenomenon not seen in the high-f_T devices. At V_{CB} = 0 and 0.5 V, F_{min} rises rapidly at the high end of the I_C range. The onset of this rise is delayed as V_{CB} increases, disappearing by V_{CB} = 1 V. This behavior is due to the large V_{CB} dependence in the onset of the Kirk effect, observed in Fig. 3 and absent in the high-f_T variant. Thus, while the high-f_T device is limited to V_{CB} values in the 0 to 1 V range for best F_{min}, the enhanced-breakdown device is best suited for operation with V_{CB} between 1 and 2 V, a 1 V shift.

The implications toward gain for this shift in optimum V_{CB} range are illustrated in Figs. 9 and 10, which plot G_A vs. I_C for the high-f_T and enhanced-breakdown devices over the same conditions considered above. We note the impact of early Kirk onset in the form of reduced G_A in the enhanced-breakdown device at V_{CB} below 1 V. More significantly, we note that the gain improves as a function of V_{CB} in both devices, due to the decrease in C_{CB} that accompanies the increased depletion into the collector. Both variants show similar G_A values at higher V_{CB}. However, since the high-f_T device experiences a large amount of F_{min} degradation at such V_{CB} values, designers would avoid these biases. Thus, the enhanced-breakdown device enjoys an advantage in gain resulting from its ability to leverage higher V_{CB} without F_{min} degradation.

To better understand the mechanism by which F_{min} degrades with V_{CB}, particularly in the high-f_T device, we consider the behavior of I_B. Since holes generated by impact ionization are known to exit the base as a negative current, I_B is a measure of the magnitude of avalanche within the device. Fig. 11 plots I_B vs. I_C for the same V_{CB} steps explored in the discussion above. We note that I_B is positive and independent of V_{CB} at values below 1 V. This is the normal forward bias regime in the absence of avalanche. At V_{CB} values of 1 V and higher, however, I_B becomes negative and increases in magnitude with both increasing V_{CB} (higher electric field) and increasing I_C (more electrons to initiate impact ionization). Indeed, the increase mirrors that of F_{min}, suggesting that the noise figure degradation is a direct result of avalanche.

We explore this connection further by plotting the change in F_{min} on a linear scale (rather than in dB) vs. the change in base current, with both quantities referenced to their V_{CB} = 0 values. Fig. 12 shows such a plot for I_C = 5 mA. We observe a strong linear dependence, indicating that the increase in F_{min} is the direct result of avalanche.

IV. CONCLUSIONS

The ability to create multiple variants within a SiGe HBT family allows tailoring by application. In particular, a modified-collector device variant with higher breakdown and lower C_{CB} and R_B allows not only for improved F_{min} at lower V_{CB} but also operation at higher V_{CB} bias for improved gain without noise degradation due to avalanche. Such a device improves the flexibility of IBM's 200 GHz SiGe HBT technology and suggests great promise for the realization of low-noise circuits in silicon, competitive with GaAs HEMT technologies at the higher frequencies of a variety of emerging wireless applications.

ACKNOWLEDGMENTS

The authors thank Dale Jadus, Scott Parker and their teams for the use of their measurement facilities as well as the members of the SiGe development teams for access to the latest process.

REFERENCES

[1] G. Freeman, M. Meghelli, Y. Kwark, S. Zier, A. Rylyakov, M.A. Sorna, T. Tanji, O. Schreiber, K. Walter, J.-S. Rieh, B. Jagannathan, A. Joseph and S. Subbanna, "40 Gb/s circuits built from a 120 GHz f_T SiGe technology," *IEEE J. Solid State Circuits*, vol. 37 no. 9, pp. 1106-1114, 2002.

[2] D. Greenberg, S. Sweeney, C. LaMothe, K. Jenkins, D. Friedman, B. Martin Jr., G. Freeman, D. Ahlgren, S. Subbanna and A. Joseph, "Noise performance and considerations for integrated RF/analog/mixed-signal design in a high-performance SiGe BiCMOS technology," *Tech. Dig. IEEE Int. Electron Device Meeting*, pp. 495-498, 2001.

[3] D.R. Greenberg, B. Jagannathan, S. Sweeney, G. Freeman and D. Ahlgren, "Noise performance of a low base resistance 200 GHz SiGe technology," to be presented at *IEEE Int. Electron Device Meeting*, 2002.

[4] B. Jagannathan, M. Khater, F. Pagette, J.-S. Rieh, D. Angell, H. Chen, J. Florkey, F. Golan, D.R. Greenberg, R. Groves, S. J. Jeng, J. Johnson, E. Mengistu, K.T. Schonenberg, C.M. Schnabel, P. Smith, A. Stricker, D. Ahlgren, G. Freeman, K. Stein and S. Subbanna, "Self-aligned SiGe NPN transistors with 285GHz f_{MAX} and 207GHz f_T in a manufacturable technology," *IEEE Electron Device Lett.*, vol. 23, no.5, 2002.

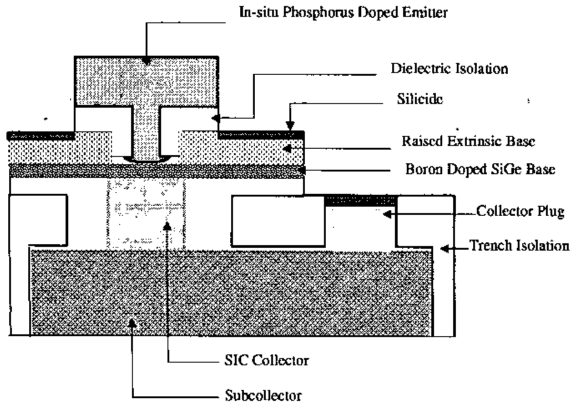

Fig. 1 - Cross-section of a high-f_T (200 GHz) raised-base SiGe HBT. An *enhanced-breakdown* variant is formed by modifying the SIC collector implant.

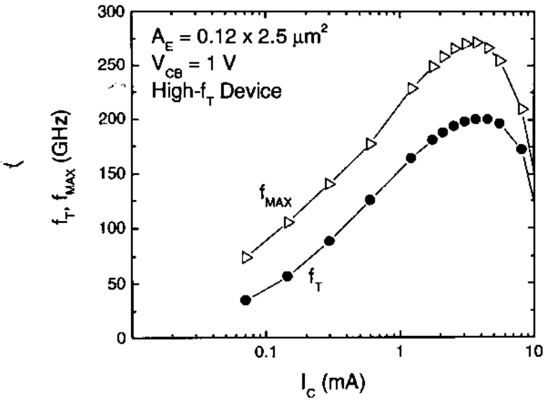

Fig. 2 - Unity current gain (f_T) and unilateral power gain (f_{MAX}) cut-off frequencies vs. collector current (I_C) for a 0.12 x 2.5 μm² *high-f_T* SiGe HBT.

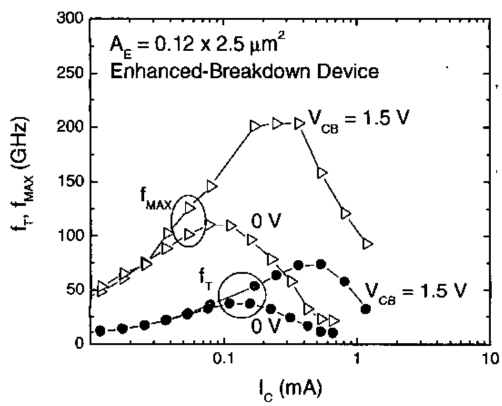

Fig. 3 - Unity current gain (f_T) and unilateral power gain (f_{MAX}) cut-off frequencies vs. collector current (I_C) for a 0.12 x 2.5 μm² *enhanced-breakdown* SiGe HBT.

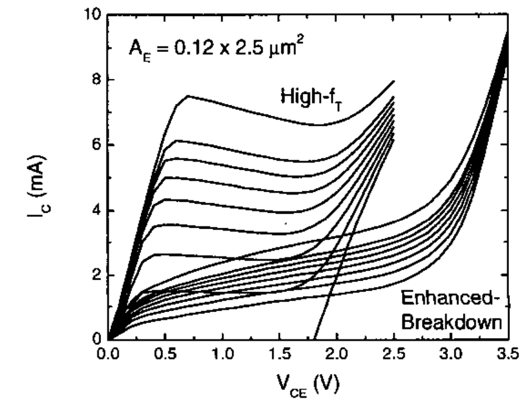

Fig. 4 - Collector current (I_C) vs. collector-emitter voltage (V_{CE}) for *high-f_T* and *enhanced-breakdown* variants of a 0.12 x 2.5 μm² SiGe HBT (BV_{CEO} = 1.8 and 2.8 V).

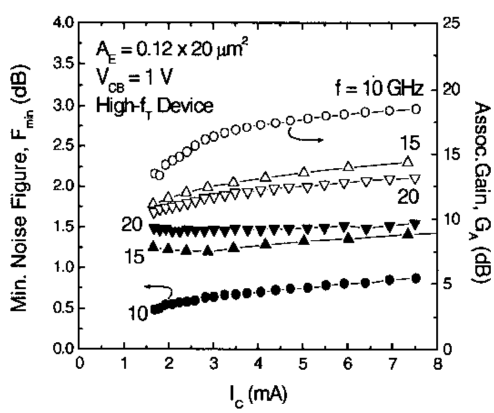

Fig. 5 - Min. noise figure (F_{min}) and assoc. gain (G_A) vs. collector current (I_C) at 10, 15 and 20 GHz and V_{CB} = 1 V for a 0.12 x 20 μm² *high-f_T* SiGe HBT.

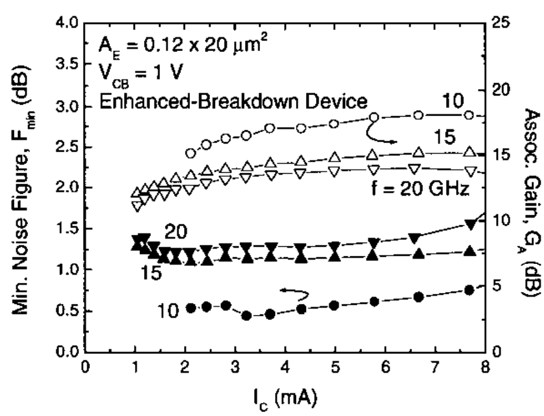

Fig. 6 - Min. noise figure (F_{min}) and assoc. gain (G_A) vs. collector current (I_C) at 10, 15 and 20 GHz and V_{CB} = 1 V for a 0.12 x 20 μm² *enhanced-breakdown* SiGe HBT.

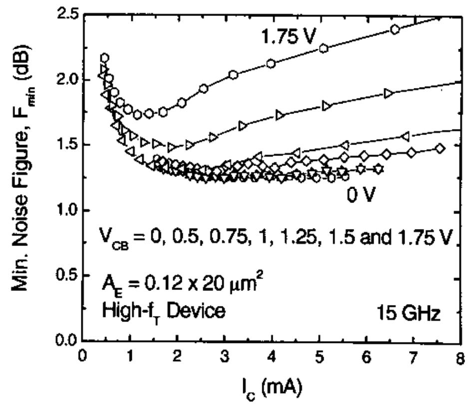

Fig. 7 - Min. noise figure (F_{min}) vs. collector current (I_C) for a 0.12 x 20 μm^2 *high-f_T* SiGe HBT at 15 GHz and V_{CB} = 0, 0.5, 0.75, 1, 1.25, 1.5 and 1.75 V.

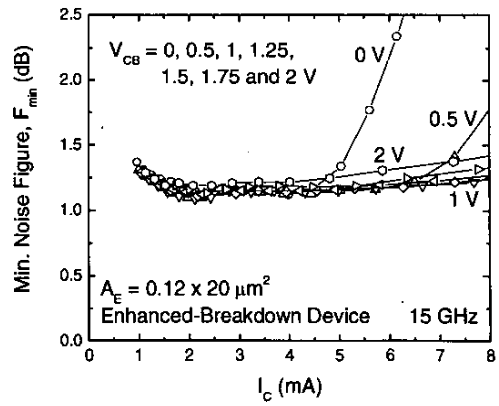

Fig. 8 - Min. noise figure (F_{min}) vs. collector current (I_C) for a 0.12 x 20 μm^2 *enhanced-breakdown* SiGe HBT at 15 GHz and V_{CB} = 0, 0.5, 1, 1.25, 1.5, 1.75 and 2 V.

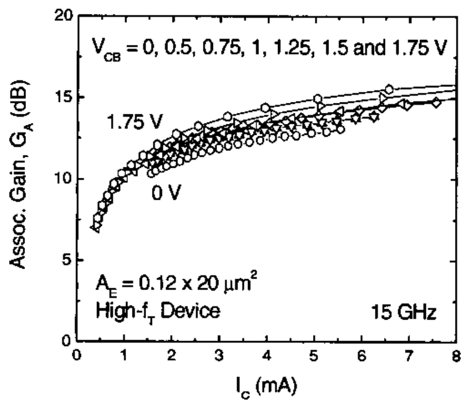

Fig. 9 - Assoc. gain (G_A) vs. collector current (I_C) for a 0.12 x 20 μm^2 *high-f_T* SiGe HBT at 15 GHz and V_{CB} = 0, 0.5, 0.75, 1, 1.25, 1.5 and 1.75 V.

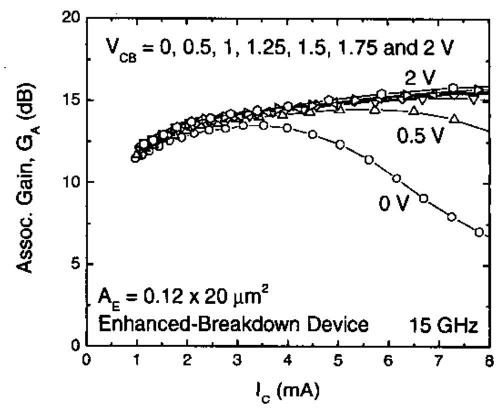

Fig. 10 - Assoc. gain (G_A) vs. collector current (I_C) for a 0.12 x 20 μm^2 *enhanced-breakdown* SiGe HBT at 15 GHz and V_{CB} = 0, 0.5, 1, 1.25, 1.5, 1.75 and 2 V.

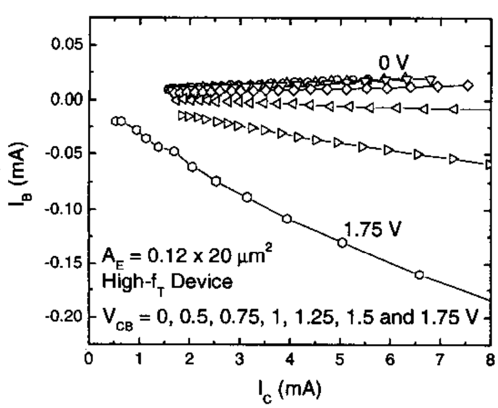

Fig. 11 - Base current (I_B) vs. collector current (I_C) for a 0.12 x 20 μm^2 *high-f_T* SiGe HBT at V_{CB} = 0, 0.5, 0.75, 1, 1.25, 1.5 and 1.75 V, showing I_B reversal.

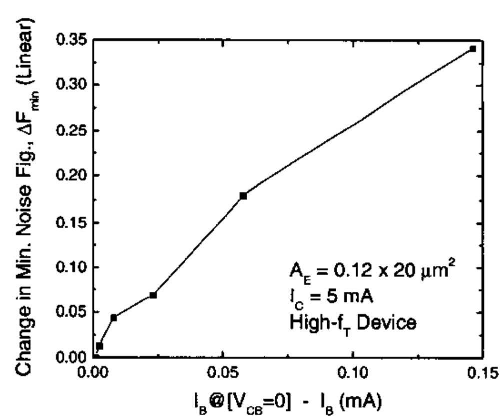

Fig. 12 - Change in min. noise figure (ΔF_{min}) on a linear scale vs. avalanche-induced I_B (I_B in excess of V_{CB} = 0 value) at I_C = 5 mA, indicating a strong correlation.